International Journal of High-Rise Buildings
December 2020, Vol 9, No 4, 361-368
https://doi.org/10.21022/IJHRB.2020.9.4.361

International Journal of
High-Rise Buildings
www.ctbuh-korea.org/ijhrb/index.php

Design Method of Steel Slit Shear Walls with Tapered Links for Structural Condition Assessment

Liusheng He[1,2], Chen Wu[1,2], and Huanjun Jiang[1,2]

[1]*State Key Laboratory of Disaster Reduction in Civil Engineering, Tongji University, China*
[2]*Department of Disaster Mitigation for Structures, Tongji University, China*

Abstract

The authors developed a new type of steel slit shear wall (SSSW) having the function of structural condition assessment through visually inspecting the out-of-plane deformation of the designed tapered links subjected to lateral deformation. To facilitate its practical application, this paper studies how to design dimensions of the tapered links. Two parameters, the width-to-thickness ratio of the tapered links and steel yield stress, were studied. The performance of structural condition assessment was affected by both parameters with the width-to-thickness ratio being the controlling one. Through both numerical and experimental study, the designed width-to-thickness ratio of tapered links for different levels of structural condition assessment was established considering the effect of different steel grades used. In practice, the dimensions of tapered links can be determined following the design equation provided. Finally, a design procedure for the proposed SSSW system is provided.

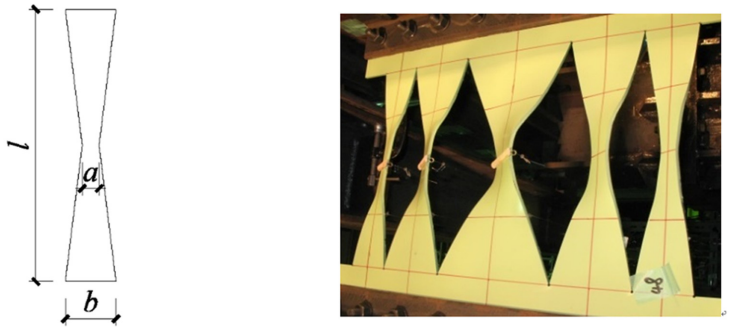
Keywords: Steel slit shear wall, structural condition assessment, energy dissipation, width-to-thickness ratio, out-of-plane deformation

1. Introduction

To mitigate the damage of the main structure system in case of devastating earthquakes, energy dissipating devices are often used to harvest the seismic damage. In the past several decades, quite several energy dissipating devices have been developed, such as viscous fluid damper, viscoelastic solid damper, metallic damper, friction dampers, et al. Among them, the metallic damper is one of the most widely adopted types, due to the performance efficiency with relatively low cost.

Belong to the category of metallic dampers, the steel slit shear wall (SSSW) has attracted much attention since its initial appearance. Kobori et al. (1992) proposed a new steel shear wall with honeycomb-shaped holes, which may be considered as the first SSSW. More people tend to believe that Hitaka and Matsui (1998) started the pioneer work on SSSWs. Through experimental study, they established the formulae for primary mechanical property, influence of slit configuration and stiffeners (Hitaka and Matsui 2003). After their work, more researchers began to work on SSSWs (Ma et al. 2010, Cortes and Liu 2011, Ke and Chen 2012). In these studies, the focuses are either improved hysteresis behavior with using out-of-plane constrainers, or design method. Jacobsen et al. (2010) started to work on SSSWs for the purpose of structural condition assessment by observing the out-of-plane deformation of rectangular links separated by vertical slits. Their concept was found feasible while difficulty existed to judge the occurrence of the out-of-plane deformation with small amplitude. In addition, the fracture at slit ends was still an issue unsolved. As the improvement, Kurata et al. (2015) worked on another new SSSW for the purpose of structural condition assessment. Different from the work of Jacobsen et al. (2010) using rectangular links, variable-section links formed by cutting diamond-shaped holes in the steel plate were used. The SSSW with tapered links is illustrated in Figure 1. The end section width of the tapered link is three times the width of the middle section ($b = 3a$). The advantages of using tapered shape for the links include: (1) firstly larger out-of-plane deformation making it easier to observe with the naked eye; (2) elimination of fracture at slit ends. SSSWs with tapered links give amplitude of out-of-plane defor-mation over 1.5 times that of SSSWs with rectangular links. The tapered shape accommodates the stress distribution along the height and the largest stress is not developed at slit ends which eliminates the potential fracture thereby. For the purpose of structural condition assessment, tapered links with different width-to-thickness ratios corresponding to different levels of lateral drifts to monitor can be designed. Subjected to lateral deformation, the tapered link with a larger width-to-thickness ratio deforms out of plane earlier and larger. For instance, the middle widest link in Figure 1(b) deforms out of plane first. By visually observing the sequence of out of plane deformed tapered

†Corresponding author: Jiang, Huanjun
Tel: 86-21-65986151, Fax: +86-21-65982668
E-mail: jhj73@tongji.edu.cn



(a) a tapered link (b) a SSSW with three different links (Kurata et al. 2015)

Figure 1. SSSW with tapered links.

links, quick estimation of the structural condition in terms of the experienced maximum lateral drift can be made.

SSSWs with tapered links have been found applicable for the function of structural condition assessment (Kurata et al. 2015, He et al. 2015). It has been confirmed that the width-to-thickness ratio of the tapered link controls the initiation of notable out-of-plane deformation. However, a design method for the tapered link is still missing for practical application. More specifically, given the target lateral deformation to monitor, the required width-to-thickness ratio of tapered links needs to be given. Also, different steel grades may be used for manufacturing SSSWs with tapered links and thus the influence of steel yield stress needs to be considered in deriving the design equations.

To summarize, this paper aims to establish the design method of tapered links for assessing different levels of inter-story drift representing different structural conditions. To investigate the influence of steel yield stress, parametric analysis was conducted. For experimental validation, two SSSW specimens using two different steel grades were designed and tested under reversed cyclic loading. Test results regarding strength and stiffness, development of out-of-plane deformation were discussed in detail.

2. Mechanical property of SSSWs

2.1. SSSWs with Tapered Links

A schematic of a tapered link is illustrated in Figure 1(a), where a, b and l denote the middle section width, end section width, and link height, respectively. The ratio of end section width to middle section width being 3 produces plastic hinge formed at the quarter height of the link. With the assumption of full plasticity developed at the quarter-height section, plastic strength can be estimated as follows (Kurata et al. 2015):

$$Q_p = \frac{4a^2 t}{l} f_y \tag{1}$$

where f_y is the yield stress; t is the plate thickness.

The elastic stiffness of the tapered link is determined by the following equation (Kurata et al. 2015):

$$K = \frac{1}{\frac{1}{12.7Et}\left(\frac{l}{a}\right)^3 + \frac{0.55l}{Gat}} \tag{2}$$

where E is the Young's modulus; G is the shear modulus

Based on Eq. (1) Eq. (2), summation of all tapered links gives the wall's overall shear strength and stiffness respectively.

2.2. SSSWs with Rectangular Links

A rectangular link's shear strength is provided by the plasticity developed at two ends as follows (Hitaka and Matsui 2003):

$$Q_p = \frac{2M_p}{l} = \frac{tb^2 t_y}{2l} = \frac{btf_y}{2\alpha} \tag{3}$$

where $M_p = b^2 t / 4f_y$ is the moment at link ends when full plasticity occurs; b is link width; l is link length; t is thickness; f_y is yield stress; and $\alpha = l / b$ is the aspect ratio of the link.

The elastic stiffness of an SSSW with rectangular links is estimated by summing up all contributions from individual links (both the shear and flexural deformation) and unslitted portion (shear deformation) , as given below:

$$K = \frac{1}{\frac{1.2l}{GBt} + \gamma\frac{l^3}{Etb^3}} \tag{4}$$

where $\gamma = (1 + 1 / \alpha)$ is a multiplier that reflects the flexibility at the ends of the flexural links, with $\gamma = 1$ denoting perfectly rigid and otherwise $\gamma > 1$; and B is the width of the unslitted portion.

Based on Eq. (3) and Eq. (4), summation of all rectangular links gives the wall's overall shear strength and stiffness respectively.

3. Parametric Analysis

Previous study showed that the initiation and growth of out-of-plane deformation of the taped link is primarily controlled by the width-to-thickness ratio ($2a/t$) but little affected by the aspect ratio (l/b) if the link is neither too short nor too long (Kurata et al. 2015). By designing tapered links of different width-to-thickness ratios in one SSSW, the structural condition assessment through inspecting the sequential occurrence of notable out-of-plane deformation of tapered links was found applicable. In addition, considering the randomness nature of the earthquake loading, the effectiveness of the tapered link in the assessment of structural condition under various types of loading was proved both numerically and experimentally (He et al. 2015). In designing dimensions of tapered links for structural condition assessment, the incremental two-cycle loading protocol can be used.

3.1. FE Model and Validation

The influence of steel yield stress on the initiation and growth of out-of-plane deformation of tapered links is investigated through parametric analysis using a commercial finite element (FE) code, ABAQUS. In the FE model, three-dimensional four-node shell element with reduced integration (S4R) is adopted. Horizontal in-plane shear displacement is applied to the top end of the tapered link with its bottom end fixed (see Figure 2(a)). The effect of initial imperfection was simulated by placing a displacement field associated to the first mode to the originally perfect-in-plane model.

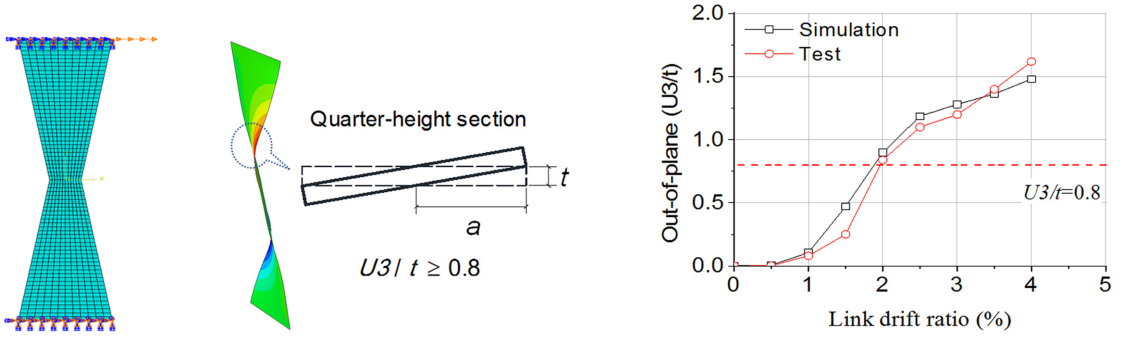
Before conducting parametric analysis, the reasonableness of the FE model was verified using previous test data. The tapered link with dimensions of $a / t / l = 30/4.3/360$ mm was used. More details regarding the tested specimens can be found in the work of He et al. (2015). Figure 2 shows the comparison between simulation and test results. It is worth mentioning that the out-of-plane deformation at the edge of the quarter-height section, where large plasticity concentrates, is used as the index to quantify the amplitude of out-of-plane deformation of the tapered links. With reference to the experimental observation, when the amplitude of out-of-plane deformation at the edge of the quarter-height section is larger than half the plate thickness, the out-of-plane deformation of the tapered link is quite notable. For quantification, the threshold value of normalized out-of-plane deformation (amplitude of out-of-plane deformation divided by plate thickness, $U3/t$) of 0.8 is determined as the criterion for judging the occurrence of notable out-of-plane deformation. For instance, the tapered link in Figure 2(c) can be used to monitor the lateral deformation of 2% link drift ratio. The fair agreement between the simulation and test results confirms that the adopted FE model can capture the initiation and development of out-of-plane defor-mation of tapered links.

3.2. Analysis Results

16 tapered links with different dimensions were built: link height of 310 mm; middle section widths of 18, 24, 30, and 36 mm respectively; plate thicknesses of 3, 3.5, 4, and 4.5 mm respectively. The resulting width-to-thickness ratios ranged between 8 and 24. Four steel grades were considered, with yield stress of 235 MPa, 345 MPa, 460 MPa and 690 MPa respectively. Thus, the total number of FE models analyzed was 64.

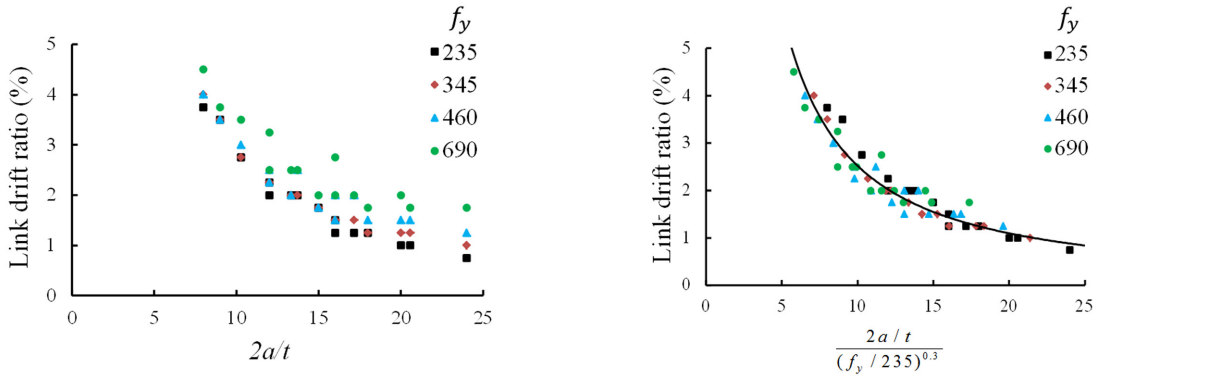
Figure 3 shows the simulated results. The ordinate of link drift ratio is the normalized link's lateral deformation (net shear deformation experienced by the link divided by link height) when notable out-of-plane deformation occurs. As discussed previously, the width-to-thickness ratio controls the initiation and development of out-of-plane deformation. With abscissa being width-to-thickness ratio ($2a / t$) in Figure 3(a), however, the data is quite scattered. To consider the influence of steel yield stress, it is reasonable to include the parameter of yield stress in the controlling width-to-thickness ratio. Using abscissa being the normalized width-to-thickness ratio ($(2a / t / (f_y / 235)^{0.3}$) in Figure 3(b) makes the data discreteness much improved.

Through regression analysis of the obtained data, Eq. (5) can be used to establish the relationship between the



(a) FE model (b) index of out-of-plane deformation (c) comparison between test and simulation

Figure 2. Verification of FE model.



(a) drift ratio versus width-to-thickness ratio (b) drift ratio versus normalized width-to-thickness ratio

Figure 3. Simulation results of parametric analysis.

target link drift ratio Δ when notable out-of-plane deformation occurs and the width-to-thickness ratio of the tapered link considering the influence of yield stress.

$$\Delta = 35\left(\frac{2a/t}{(f_y/235)^{0.3}}\right)^{-1.2} \tag{5}$$

4. Test Preparation

4.1. Design of Test Specimens

The prototype structure with the installed SSSWs is a medium-rise steel moment frame building with a story height of 3300 mm. The specimens are designed as 1/5 scaled, which gives an overall specimen height of 660 mm. Along the height, the middle portion with slits is determined to occupy about half. Two specimens are designed and share the identical overall dimensions of 660 mm by 720 mm and the only difference is the steel material used. The steel plate used to manufacture the specimens is the common mild carbon steel and of the same thickness of 3.8 mm by physical measurement. From the standard tensile coupon tests, yield stress of $f_y = 346$ MPa and ultimate strength of $f_u = 494$ MPa are obtained for Specimen 1. For Specimen 2, yield stress of $f_y = 473$ MPa and ultimate strength of $f_u = 606$ MPa are obtained.

Figure 4 shows the detailed dimensions. Three tapered links with different widths are included in each specimen, with the largest end section width of 90 mm (Link 1), second largest end section width of 72 mm (Link 2) and smallest end section width of 54 mm (Link 3). The ratio of end section width to middle section width is remained as 3. To have a relatively wide wall to prevent the early global plate buckling, narrow rectangular links with a width of 20 mm, which behaves mainly in plane due to the small width-to-thickness ratio, are added. In each specimen, the circles at both top and bottom portion are the openings for bolting to the loading frame.

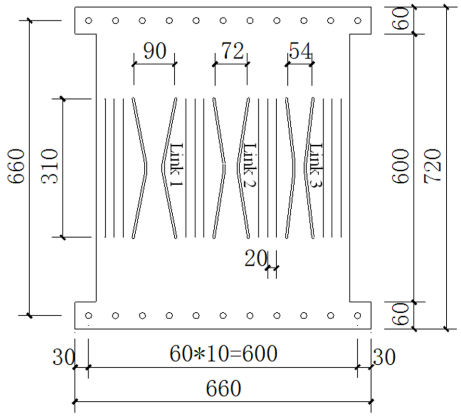
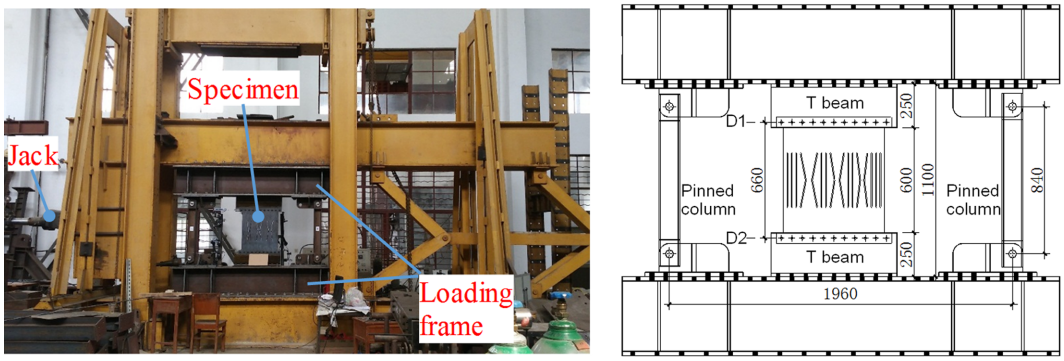


Figure 4. Dimensions of Specimen 1 and Specimen 2.

4.2 Test Setup, Instrumentation and Loading Protocol

The test setup is a mega portal frame as shown in Figure 5(a). To accommodate the relatively small specimens, an inner loading frame was built inside, with details of which shown in Figure 5(b). Two T-shaped beams (250 × 9 × 14 mm) connect the load frame and specimens. High-strength bolts are used in the connection between the specimen and T-shaped beam.

The lateral deformation applied to the specimen is controlled by the jack. The net shear deformation concentrated on the middle specimen is measured by attaching two displacement transducers along the bolting line, as shown in Figure 5(b). For instance, the difference between the readings of displacement transducers D1 and D2 is calculated as the net shear deformation for the specimen. During the loading process, the displacement of the jack is carefully tuned to reach the desired net drift ratio of the specimen. To measure the out-of-plane deformation of tapered links, displacement transducers were placed in the direction perpendicular to the plane of the link and attached by wire to edges of the quarter-height section. The out-of-plane deformation was calculated using the transducer readings considering geometric relation.



(a) photo in test (b) close view (Unit: mm)

Figure 5. Test setup.

The loading protocol was the same as previously adopted, the incremental two-cycle loading with each amplitude repeated twice. The amplitude increment is 0.25%.

5. Test Results and Discussions

5.1. Mechanical Behavior

According to the respective equations in Section 2, the summation of all tapered links and rectangular links gives the wall's overall strength and stiffness respectively. Table 1 lists the obtained test results and comparison with calculation. The theoretical calculation of plastic strength Q_p is based on the full plasticity assumption. While, due to the occurrence of out-of-plane deformation, the tested maximum shear strength $Q_{max,t}$ was smaller than prediction by about 20%. The tested elastic stiffness K_t was nearly 90% of the calculation. The around 10% error was attributed to the flexibility of T-shaped beam in the connection. Another potential cause of this error might be the non-rigid bolting connection between the specimen and T-shaped beam.

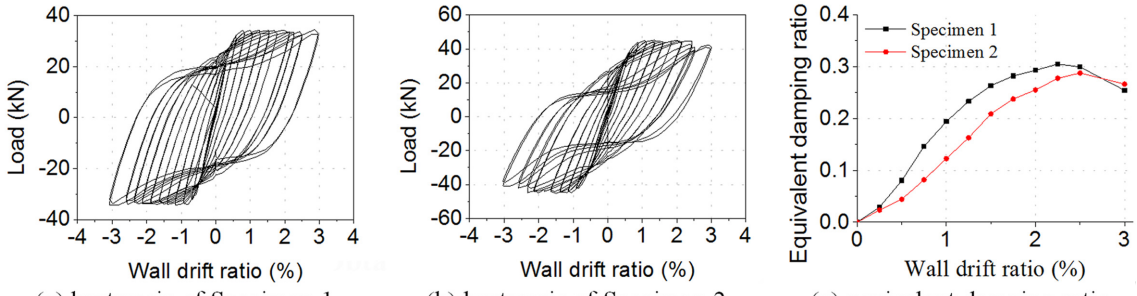
Figure 6 shows the obtained hysteretic curves and equivalent damping ratios of both specimens. Specimen 1 used relatively low yield stress steel with larger ductility than that of Specimen 2, which gave the plumper hysteresis of Specimen 1. The equivalent damping ratio was estimated using the standard procedure for both specimens at each drift amplitude. Within the wall drift ratio of 2.5%, the equivalent damping ratio of Specimen 1 was larger than that of Specimen 2, revealing its better energy dissipation capacity. Both specimens reached the maximum equivalent damping ratio around 0.3 at similar wall drift ratio.

5.2 Out-of-plane Deformation

The out-of-plane deformation of tapered links at the edge of quarter-height section was measured by displacement transducers. Figure 7 shows the observed out-of-plane deformation of Specimen 1. As expected, three tapered links in Specimen 1 presented much more notable out-of-plane deformation than the surrounding rectangular

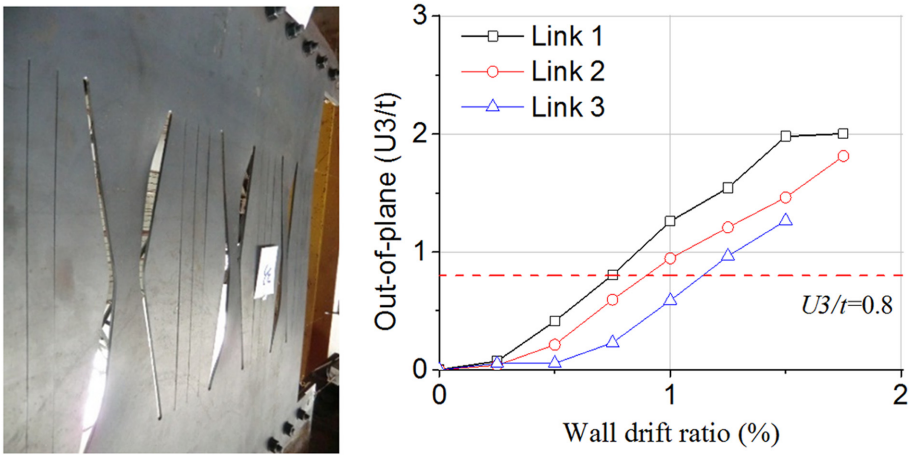
Table 1. Strength and stiffness

Specimen	Q_p (kN)	$Q_{max,t}$ (kN)	$Q_{max,t}/Q_p$	K (kN/mm)	K_t (kN/mm)	K_t/K
1	44.1	35.4	0.80	16.3	14.3	0.88
2	60.3	47.4	0.79	16.3	14.5	0.89



(a) hysteresis of Specimen 1 (b) hysteresis of Specimen 2 (c) equivalent damping ratio

Figure 6. Obtained hysteresis and equivalent damping ratio.



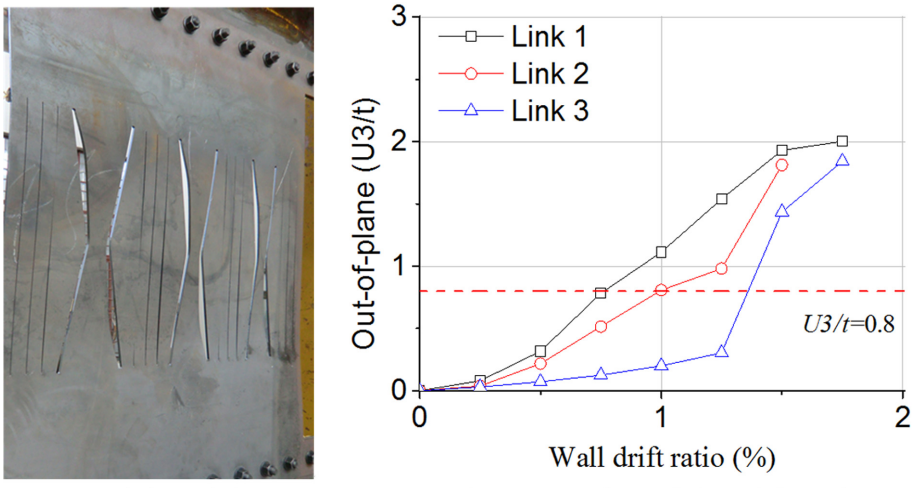
(a) deformed shape (b) progress of out-of-plane deformation

Figure 7. Out-of-plane deformation of Specimen 1.

links (Figure 7(a)), which made the visual inspection easier. As shown in Figure 7(b), three links deformed out of plane in sequence, first the widest Link 1 and last the narrowest Link 3. The controlling factor of the width-to-thickness ratio of tapered links for the out-of-plane deformation was again confirmed. According to the previously defined criterion of notable out-of-plane deformation (Figure 2(b)), three links could be used to monitor the wall drift ratios of 0.75%, 1% and 1.25% respectively.

Figure 8 shows the observed out-of-plane deformation of Specimen 2. Its out-of-plane deformation looked like that of Specimen 1. Three tapered links deformed out of plane in sequence, first the widest Link 1 and last the narrowest Link 3. According to the previously defined criterion of notable out-of-plane deformation (Figure 2(b)), three links could be used to monitor the wall drift ratios of 0.75%, 1% and 1.5% respectively. Link 1 and Link 2 of Specimen 2 deformed notably out of plane at the same wall drift ratio as those two links of Specimen 1. Only the narrowest Link 3 of Specimen 2 deformed notably out of plane a little bit later. As steel yield stress was the only difference between two specimens, it revealed that the influence of yield stress was limited.

Note that the abscissa of wall drift ratio in Figures 6-8 is defined as the lateral deformation divided by the wall height, which is different from the link drift ratio (net shear deformation experienced by the link divided by link height) in Figure 3. For a typical SSSW as shown in Figure 4, there is a height difference between the wall and link, which gives amplified link drift ratio for the link. With the wall height being two times the link height, the resultant link drift ratio is amplified by two times ignoring the small in-plane shear deformation of the wall portion without slits. For instance, three links of Specimen 1 buckled notably out of plane at wall drift ratios of 0.75%, 1% and 1.25% respectively; we could also say that three



(a) deformed shape (b) progress of out-of-plane deformation

Figure 8. Out-of-plane deformation of Specimen 2.

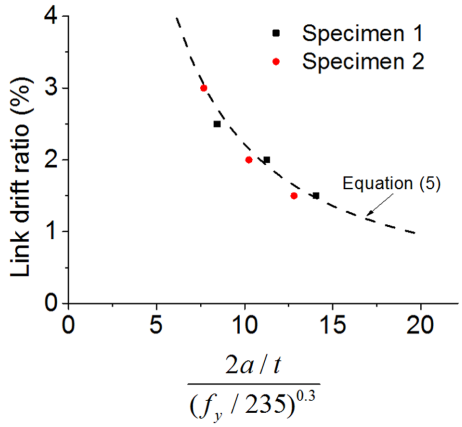


Figure 9. Comparison between prediction and test.

links buckled notably out of plane at link drift ratios of 1.5%, 2% and 2.5% respectively. For Specimen 2, three links buckled notably out of plane at link drift ratios of 1.5%, 2% and 3% respectively.

Out of the parametric analysis, Eq. (5) was derived to establish the relationship between the target link drift ratio to monitor and width-to-thickness ratio of tapered links needed. To examine the rationality of Eq. (5), the tested link drift ratios when tapered links deformed notably out of plane were plotted together with it, as shown in Figure 9. It can be seen that Eq. (5) basically presented the tested scattered data well.

The narrow rectangular links surrounding tapered links in both specimens presented a stable mainly in-plane behavior, which meant good energy dissipation. The designed small width-to-thickness ratio of rectangular links of 5.3 (width of 20 mm divided by plate thickness of 3.8 mm) ensured this mainly in-plane behavior.

5.3. Design Procedures

In the scenario of practical application, the SSSW will be installed between floor beams. As demonstrated in the test, through careful design, its energy dissipation capacity could be not necessarily bad. For the purpose of structural condition assessment, thin steel plates are required to allow large out-of-plane deformation of tapered links for the easiness of visual inspection. While for the purpose of energy dissipation, the occurrence of out-of-plane deformation is not expected. Taken together, the configuration of the designed specimens as shown in Figure 4 seems like a good combination, using tapered links for the purpose of structural condition assessment while narrow rectangular links for the purpose of energy dissipation. The width-to-thickness ratio is also the key parameter to control the out-of-plane behavior of rectangular links. To ensure the mainly in-plane behavior, the rectangular links are required to be designed as narrow (equal to thick). A width-to-thickness ratio of 5.3 was adopted for the rectangular links in the study, which demonstrated their mainly in-plane behavior. And this value is also in accordance with the recommendation by Hitaka and Matsui (2003), ranging from 3 to 10.

In designing SSSWs in a building structure, the target structural condition levels of the building structure to monitor (in terms of the experience maximum drift ratio) need to be defined first. The height difference between the wall and link needs to be consider here. After confirmation of the type of steel plate to be used, Eq. (5) can be used to determine the required width-to-thickness ratio of the tapered links. With multiple targeted drift ratios to monitor, a series of tapered links can be designed. After designing tapered links for the purpose of structural condition assessment, the supplement of rectangular links can be determined according to the expectations of both elastic stiffness and shear strength at each story. In tuning the design of rectangular links to obtain the required stiffness and shear strength, the width-to-thickness ratio within the range of 3-10 is recommended to follow.

6. Conclusions

This study investigates the influence of steel yield stress on the initiation and development of out-of-plane deformation of tapered links. By parametric analysis, a design method for the tapered links used for structural condition assessment is obtained. Major findings are summarized as follows:

1. Width-to-thickness ratio is the controlling factor for the out-of-plane deformation of tapered links. Steel yield stress also affects, but the degree is limited.
2. An equation to design the dimensions of tapered links for the function of structural condition assessment is obtained. Given the target link drift ratio to monitor, the width-to-thickness ratio of tapered links with consideration of the influence of steel yield stress can be calculated.
3. Through careful design, the proposed SSSW can also have good energy dissipation capacity.
4. Considering the practical application, a procedure is provided for designing SSSWs for the purpose of both structural condition assessment and energy dissipation.

Acknowledgments

The authors are grateful for the support from National Natural Science Foundation of China under Grant No. 51608388.

References

Cortes, G., and Liu, J. (2011). Experimental evaluation of steel slit panel-frames for seismic resistance. *Journal of Constructional Steel Research*, 67: 181-191.

He, L., Kurata, M., and Nakashima, M. (2015). Condition assessment of steel shear walls with tapered links under

various loadings. *Earthquakes and Structures*, 9: 767-788.
Hitaka, T., and Matsui, C. (1998). "Strength and behavior of steel bearing wall with slits." Proc. 5th Pacific Strucutral Steel Conference, Seoul, Korea, pp. 991-996.
Hitaka, T,. and Matsui, C. (2003). Experimental study on steel shear wall with slits. *Journal of Structural Engineering*, 129: 586-595.
Jacobsen, A. (2010). Development of steel slit wall dampers with embedded condition assessment capabilities. Ph.D dissertation, Kyoto University.
Ke, K. and Chen, Y. (2012). "Design method of steel plate shear wall with slits considering energy dissipation." Proc. 15th World Conference on Earthquake Engineering, Lisboa, Portugal.
Kurata, M,. He, L., and Nakashima, M. (2015). Steel slit shear walls with double-tapered links capable of condition assessment. *Earthquake Engineering and Structural Dynamics*, 44: 1271-1287.
Kobori, T., Miura, Y., Fukusawa, E.,Yamada, T., Arita, T. and Takenake, Y. (1992). "Development and application of hysteresis steel dampers." Proc. 10th World Conference on Earthquake Engineering, Madrid, Spain, 2341-2346.
Ma, X., Borchers, E., Pena, A., Krawinkler, H., and Deierlein, G. (2010). Design and behavior of steel shear plates with openings as energy dissipating fuses. Blume Earthquake Engineering Center, TR 173, Stanford Univ., Stanford, CA.